

Interconversion Rates between Conformational States as Rationale for the Membrane Permeability of Cyclosporines

Jagna Witek,^[a] Max Mühlbauer,^[a] Bettina G. Keller,^[b] Markus Blatter,^[c] Axel Meissner,^[c] Trixie Wagner,^[c] and Sereina Riniker^{*[a]}

Cyclic peptides have regained interest as potential inhibitors of challenging targets but have often a low bioavailability. The natural product cyclosporine A (CsA) is the textbook exception. Despite its size and polar backbone, it is able to passively cross membranes. This ability is hypothesized to be due to a conformational change from the low-energy conformation in water to a “congruent” conformation that is populated both in water and inside the membrane. Here, we use a combination of NMR measurements and kinetic models based on molecular dynamics simulations to rationalize the difference in the membrane permeability of cyclosporine E (CsE) and CsA. The structure of CsE differs only in a backbone methylation, but its membrane permeability is one order of magnitude lower. The most striking difference is found in the interconversion rates between the conformational states favored in water and in chloroform, which are up to one order of magnitude slower for CsE compared to CsA.

Cyclic peptides and peptidomimetics have regained interest in the past years as potential inhibitors of important therapeutic targets, such as class B G-protein coupled receptors or protein-protein interfaces, which are difficult to target using small molecules.^[1] Peptides violate most of the conventional physico-chemical guidelines for drug-likeness, for example, Lipinski's rule of five,^[2,3] due to their size and complexity.^[4] Consequently, most peptidic drugs have a low bioavailability, which restricts the range of potential targets.^[4–6]

The passive membrane permeability of molecules is used as a key indicator to evaluate the bioavailability of potential drug candidates for pharmaceutical applications. Permeability prediction by computational means has therefore been a long-standing challenge for the chemistry community. For small organic molecules, a clear correlation exists between the size

and polarity of a compound and its membrane permeability, which can be exploited in quantitative structure-property relationship (QSPR) models.^[2,7] Alternatively, the permeation process can be modeled explicitly using molecular dynamics (MD) simulations and the solubility-diffusion theory,^[8] in which the permeability coefficient is related to the resistance by the membrane to permeation. Despite the progress in the past decades, the quantitative prediction of membrane permeability using this MD-based approach remains challenging even for very small molecules,^[9–11] due to effects like orientational freedom^[12] and fractional diffusion.^[13] Therefore, alternative methods are needed for larger and more flexible molecules such as peptides.


The natural product cyclosporine A (CsA) is an important exception to the generally low bioavailability of peptidic drugs. CsA is able to cross membranes by passive diffusion despite being a cyclic undecamer,^[14] likely due to its capability to undergo a conformational change from “open” in water to “closed” in the membrane interior.^[15] In the open conformation, the unmethylated backbone amides form hydrogen bonds (H-bonds) with the solvent,^[16] whereas they form intramolecular H-bonds in the closed conformation.^[17] The combination of cyclization and backbone-methylation pattern (seven out of 11 residues are methylated) is thereby considered essential for CsA to adopt these two distinct conformations. Following the hypothesis of a conformational change, Jacobson and co-workers developed a general computational approach.^[15,18] The method focuses solely on the closed conformation, with the underlying assumption that it is sufficiently populated in water and in rapid interconversion with other conformations. However, for larger cyclic peptides, this assumption may not always hold. In line with this, a recent application of the approach on a diverse set of compounds has shown a low performance for larger molecules.^[19] This indicates that it could be important to consider the kinetics of the conformational behaviour explicitly to improve the prediction accuracy.

A first example of such an approach was recently reported by us for CsA.^[20] In the case of CsA, the transition from the open to the closed conformation involves two processes: major changes in the backbone torsion angles of residues MeBmt-1, MeLeu-4, MeLeu-6 and Ala-7, and the *cis/trans*-isomerization of the peptide bond between residues 9 and 10 (see Figure S2 in the SI). Our Markov state models (MSMs^[21]) of CsA in water and in chloroform (CHCl₃), used as substitute for the membrane interior, suggested that these two processes occur in a concerted manner.^[20] In CHCl₃, the highest energetic barrier separated a half-open conformation with all *trans* pep-

[a] J. Witek, M. Mühlbauer, Prof. Dr. S. Riniker
Laboratory of Physical Chemistry, ETH Zürich
Vladimir-Prelog-Weg 2, 8093 Zürich (Switzerland)
E-mail: sriniker@ethz.ch

[b] Prof. Dr. B. G. Keller
Department of Biology, Chemistry, Pharmacy
Freie Universität Berlin
Takustrasse 3, 14195 Berlin (Germany)

[c] Dr. M. Blatter, Dr. A. Meissner, Dr. T. Wagner
Novartis Institutes for BioMedical Research
Novartis Pharma AG
Novartis Campus, 4056 Basel (Switzerland)

 Supporting Information and the ORCID identification number(s) for the author(s) of this article can be found under:
<https://doi.org/10.1002/cphc.201700995>.

tide bonds from the rest of the conformational space, while the second highest barrier separated a closed conformation with a *cis* 9–10 peptide bond.^[20,22] The same half-open state was also populated in water together with the closed conformation. These two conformations were thus termed “congruent” states. In water, the highest energetic barrier separated the open conformation from the rest of the conformational space. The results indicated that the closed conformation is indeed accessible in water, but that the membrane permeability of CsA may be facilitated by the presence of a second, better accessible congruent conformation.

Here, we test this hypothesis and investigate the influence of the interconversion rates using a “permeability cliff”^[23] of CsA, that is, a structurally similar compound with a large difference in permeability. Cyclosporine E (CsE) is a synthetic derivative of CsA and differs only by a missing backbone methylation of residue Val-11 (Figure 1A), whereas its permeability is one order of magnitude lower.^[24]

For CsE, the small-molecule crystal structure shows a closed conformation with three intramolecular backbone H-bonds and a *cis* 9–10 peptide bond (Figure 1).^[25] No open structure or NMR data is available in the literature. To determine the structure of CsE by NMR, measurements in tetrachlorocarbon (CCl₄) and in dimethyl sulfoxide (DMSO) were performed. The solution structure in CCl₄ with five intramolecular H-bonds resembles the crystal structure (Figure 1C). All NOE upper distance bounds in CCl₄ are fulfilled by the crystal structure except slightly the distance between the side chain of MeLeu-6 and C_α of D-Ala-8 (Figure S5 in the SI). The five intramolecular H-bonds are strong as shown by the temperature amide coefficients (Table 2). No minor conformation was observed in CCl₄. In contrast to CsA, for which no structure could be resolved in DMSO due to the presence of multiple conformations, CsE adopts a major and a minor (approx. 10%) conformation in DMSO, pointing out differences in the behavior of CsE and CsA. The major conformation of CsE in DMSO (Figure 1D) resembles the conformation in CCl₄ with five strong intramolecular H-bonds (Table 1). The minor conformation could not be resolved, but the signals indicate that it does not contain β -strands.

Next, we performed MD simulations of CsE in polar and apolar solvents using the GROMOS software package^[26] and the GROMOS 54A7^[27] force field. The crystal structure was used as closed starting structure. Due to the absence of an experi-

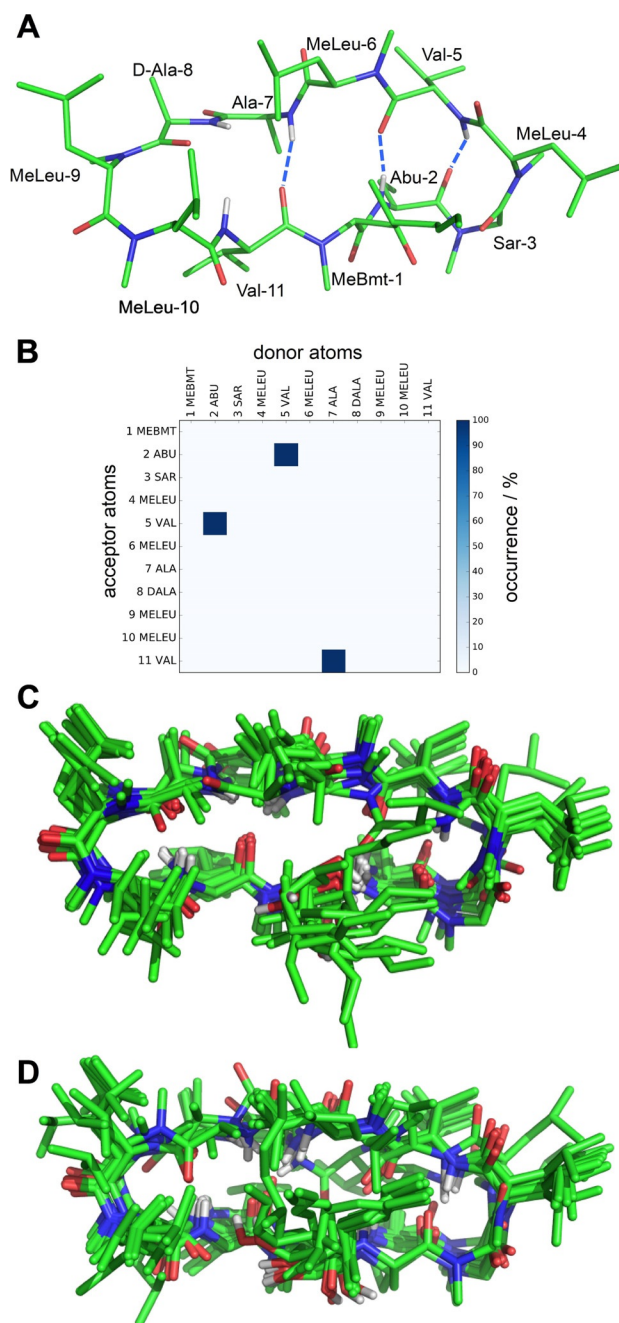


Figure 1. A) Small-molecule crystal structure of CsE (Cambridge Structure Database (CSD): SUQNUN^[25]). B) Pattern of intramolecular backbone-backbone H-bonds in the small-molecule crystal structure. C) NMR bundle of CsE in CCl₄. D) NMR bundle of CsE in DMSO.

Table 1. Temperature coefficient for the backbone amide groups of CsE in CCl₄ and DMSO.^[a]

Residue	CCl ₄ Temperature coefficient [ppb K ⁻¹]	DMSO Temperature coefficient [ppb K ⁻¹]
Abu-2	−1.7	−3.0
Val-5	−0.3	−0.9
Ala-7	−2.5	−2.5
D-Ala-8	−1.3	−1.3
Val-11	−1.4	−2.6

[a] A coefficient > −4.5 ppb K⁻¹ indicates a strong intramolecular H-bond.

mentally determined open structure of CsE, the cyclophilin-bound structure of CsA was used as starting point and modified to match the CsE topology. Initial seed conformations were obtained from standard simulations of CsE in water and in CHCl₃ as well as Hamiltonian and temperature replica-exchange simulations (HRE and TRE)^[28] in both solvents. For each solvent, 10–20 μ s of simulation data was obtained, which served as basis for the construction of the MSMs. In addition, simulations in CCl₄ and DMSO were performed for direct comparison with the NMR data.

The most striking difference between CsA and CsE was found in the time scales of the interconversion processes (Table 2). The ITS are up to one order of magnitude slower in

Table 2. Relative implied time scales (ITS) for the slowest interconversion processes of the Markov state models (MSM) in CHCl_3 , water and DMSO for CsA and CsE.^[a]

Process	CsA ^[b] CHCl_3	Water	CsE CHCl_3	Water	DMSO
1	1.25	1.0	4.0	8.75	18.0
2	0.5	0.75	3.5	3.5	3.5
3	–	0.45	2.0	2.0	1.5

[a] The ITS are given relative to the slowest process of CsA in water (shown in *italic*). The lagtime was chosen as $\tau = 12.5$ ns. [b] Values taken from Ref. [20]. Note that a factor five was missing for the ITS originally reported in Ref. [20].^[29]

the case of CsE. In CHCl_3 , three slow processes were observed for CsE, thus the microstates were grouped into four metastable sets C1–C4 (Figure 2). C1 was separated from the rest of the conformational space by the highest energy barriers, leading to the slowest interconversion rate to all other metastable sets, and presents a closed conformation with five intramolecular backbone H-bonds (Figure 2B) and a *cis* 9–10 peptide

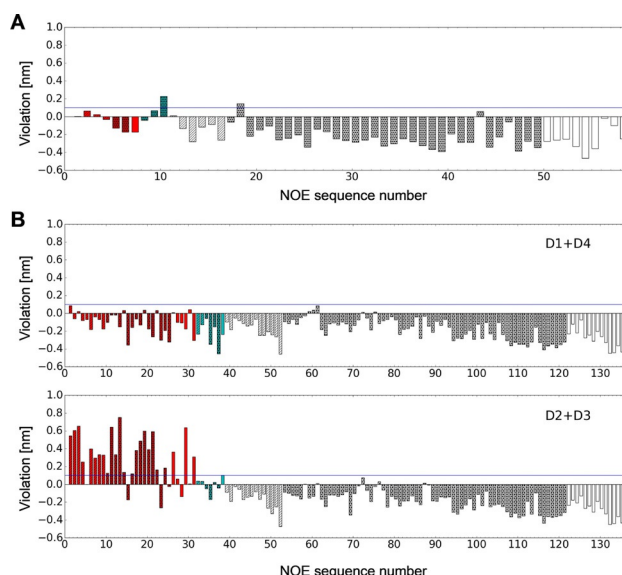


Figure 3. A) Violations of the experimental NOE upper distance bounds in CCl_4 by the 10 μs of simulation of CsE in CHCl_3 . B) Violations of the experimental NOE upper distance bounds in DMSO by the 20 μs of simulation of CsE in DMSO. The metastable sets D1 and D4 (top) and sets D2 and D3 (bottom) are combined. The NOE distances are grouped into “intercycle” (red), “intermediate” (cyan) and “vicinal” (white), and labeled as backbone-backbone (stripes), backbone-side chain (dot) and side chain-side chain (plain).

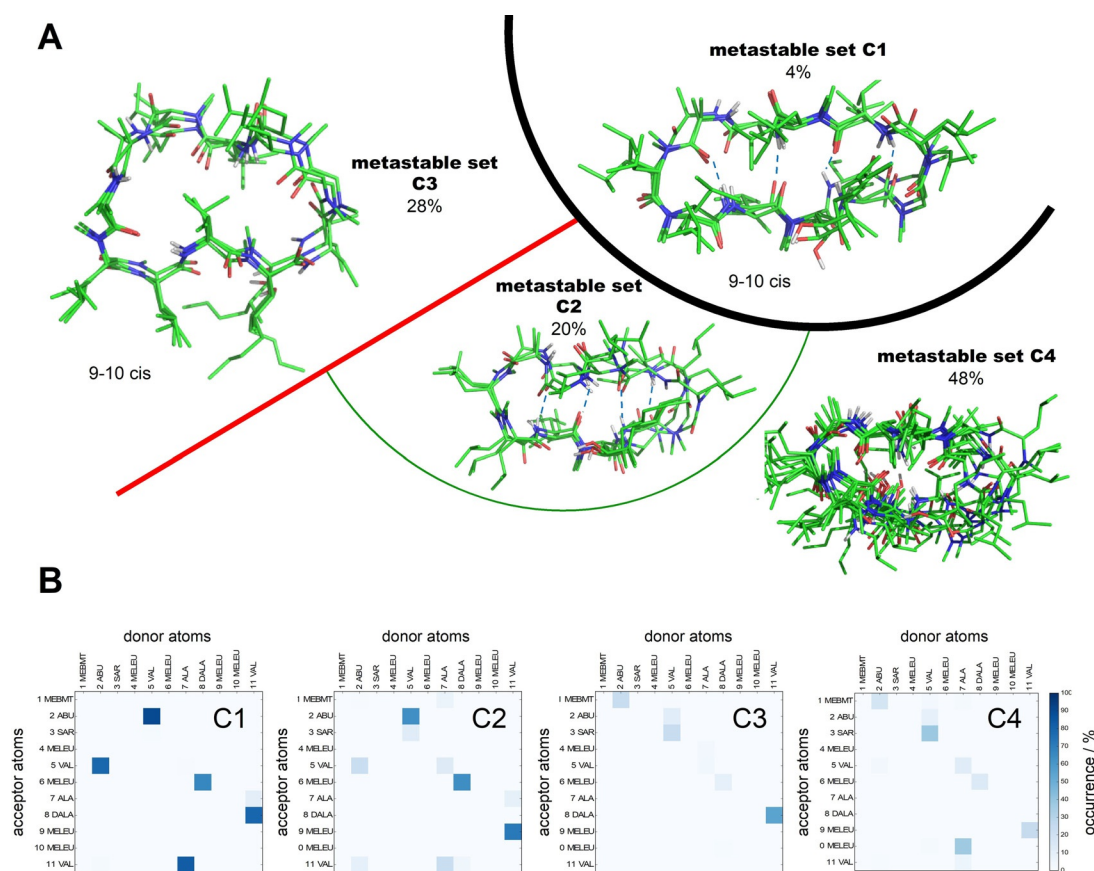


Figure 2. A) Schematic representation of the metastable sets C1, C2, C3 and C4 in CHCl_3 . The colors of the dividing lines correspond to the ITS (see Figure S6 in the SI). The structures shown are the cluster centroids of the two most abundant microstates in C1, C2 and C3 and of the seven most abundant microstates in C4. B) Pattern of intramolecular backbone H-bonds.

bond. C3 with the next slower interconversion rate contains open conformations with the 9–10 peptide bond primarily in *cis*-conformation. About half the conformations in C3 exhibit a backbone H-bond between D-Ala-8 and Val-11, which occurs also in the NMR structure. C2 presents a second closed conformational state with three dominant backbone H-bonds and a *trans* 9–10 peptide bond. C4 contains all remaining microstates and was therefore not analyzed in detail. In the case of CsE, the two processes involved in the interconversion from open to closed or *vice versa* (i.e. major changes in the backbone torsion angles and isomerization of the 9–10 peptide bond) are separated. This is in contrast to CsA, where these two processes occur in a concerted manner. The complete simulated ensemble in CHCl_3 fulfills the NOE distances (Figure 3A). The MSM in CCl_4 is similar to the MSM in CHCl_3 (see Figure S11 in the SI).

In polar solvents, the interconversion rates were the slowest (Table 2). The MSM of CsE in water is characterized by four metastable sets W1–W4 (Figure 4), where W4 contains all the remaining microstates and was therefore not analyzed in detail. W3 was separated from the rest of the conformational space by the highest energy barrier (Figure 4A). In W3, CsE adopts an open conformation without any intramolecular H-

bond and with a *trans* 9–10 peptide bond. W1 and W2 are separated from W4 by the next slowest interconversion rate and present the closed conformation with four intramolecular H-bonds and one H-bond with the solvent. W1 and W2 differ in the conformation of the 9–10 peptide bond, that is, *cis* in W1 and *trans* in W2. Again, the change in the backbone torsion angles and the isomerization of the 9–10 peptide bond occur separately. While the two processes had similar time scales in CHCl_3 , the first process is substantially slower than the second in water (Table 2). For CsA, we had hypothesized that the half-open congruent conformation, which is better accessible in water than the closed conformation, may facilitate membrane permeability. For CsE, only the pairs of closed conformations (C1/W1 and C2/W2) were observed as congruent states, which both have a low accessibility in water due to the high energy barrier separating them from the open conformation. This means that the permeability of CsE cannot be facilitated by an alternative congruent conformation with a better accessibility in the aqueous environment.

Due to the low solubility of CsE in water, DMSO had to be used as a substitute polar solvent for the NMR experiments. In contradiction to the MSM in water, these measurements showed the closed conformation as major conformation. As

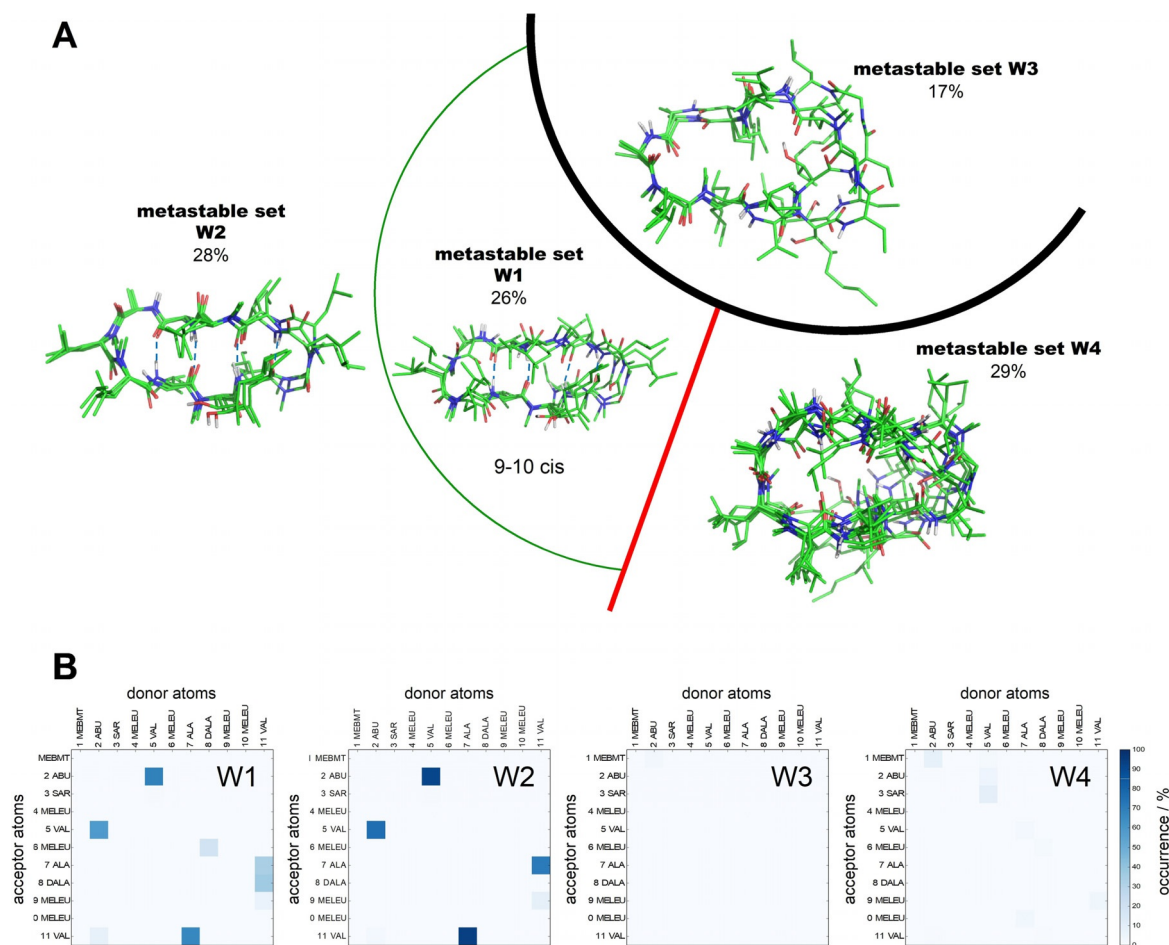


Figure 4. A) Schematic representation of the metastable sets W1, W2, W3 and W4 in water. The colors of the dividing lines correspond to the ITS (see Figure S6 in the SI). The structures shown are the cluster centroids of clusters of the two most abundant microstates in W1, W2 and W3 and of the seven most abundant microstates in W4. B) Pattern of intramolecular backbone H-bonds.

DMSO cannot serve as H-bond donor and has a significantly higher viscosity than water, it may impact the conformational behavior and interconversion rates of cyclic peptides. We therefore performed simulations of CsE in DMSO, demonstrating that the MSM in DMSO differs substantially from the MSM in water (Figure 5) and is in good agreement with the NMR data. The highest energy barrier in DMSO was found to be substantially higher than in water (Table 2) and separates the metastable set D1 with a closed conformation and a *trans* 9–10 peptide bond from the rest of the conformational space. D4 corresponds to the closed conformation with a *cis* 9–10 peptide bond. The metastable sets D1 and D4 combined fulfill the NOE distance bounds of the major conformation in DMSO (Figure 3B). We hypothesize that D2 with an open conformation represents the minor conformation observed by NMR. These results indicate that the conformational landscapes of compounds like CsE may be different in DMSO than in water, and thus experimental observations obtained in DMSO may not be directly transferable.

For the interconversion rates to be a dominant factor for membrane permeability, the time scales must be slower than membrane entrance, crossing and exit. Experimentally, it is not

possible to distinguish these steps. Although the effective permeability measured using PAMPA are given in [cm s^{-1}], it is obtained by determining the peptide concentration in the donor and acceptor compartment after a fixed incubation period,^[30] and thus does not provide information about the rate-limiting step. As CsA and CsE have the same size and adopt a similar closed conformation in apolar environment, it can be assumed that they enter, cross and leave the membrane at similar rates. Thus, their difference in permeability likely stems from the behavior in water.

In conclusion, the difference in the time scales of the interconversion processes between the permeability-cliff pair CsA and CsE of up to one order of magnitude together with the absence of an alternative congruent conformation may serve as a rationale for the lower membrane permeability of CsE. Our study highlights the importance of kinetic aspects for understanding the conformational behavior of larger cyclic peptides and for the prediction of the ability of such compounds to permeate membranes. Future work will be dedicated to the development of a design principle for permeable cyclic peptides for pharmaceutical applications.

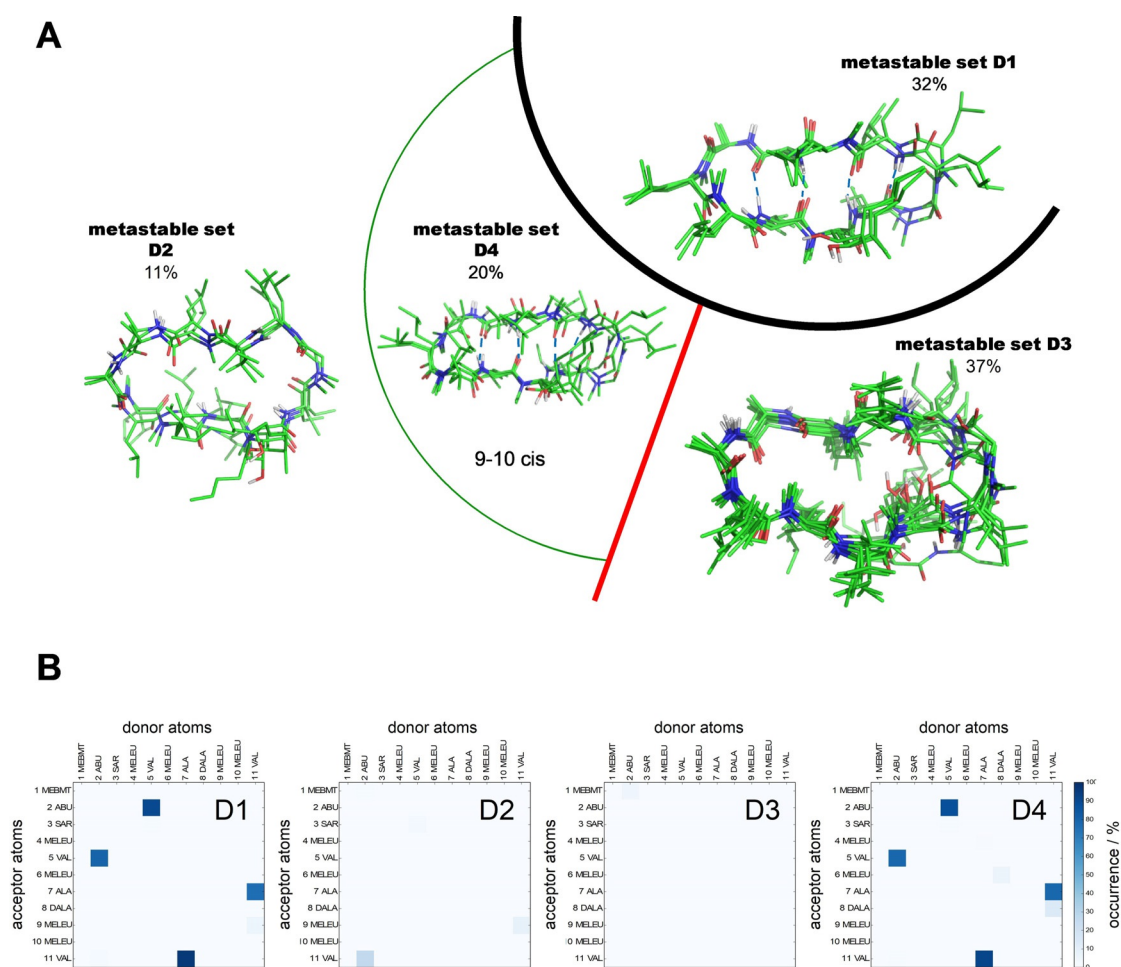


Figure 5. A) Schematic representation of the metastable sets D1, D2, D3 and D4 in DMSO. The colors of the dividing lines correspond to the ITS (see Figure S6 in the SI). The structures shown are the cluster centroids of the two most abundant microstates in D1, D2 and D4 and of the seven most abundant microstates in D3. B) Pattern of intramolecular backbone H-bonds.

Experimental Section

Details on NMR sample preparation, data acquisition and processing, structure calculation of the NMR bundles, as well as simulation details are given in the SI.

Acknowledgements

S.R. and J.W. acknowledge financial support by the Swiss National Science Foundation (Grant Number 200021-159713) and by ETH Zürich (ETH-08 15-1). B.G.K. acknowledges support by the DFG collaborative research center CRC 765, Project C10.

Conflict of interest

The authors declare no conflict of interest.

Keywords: cyclosporine • kinetics • Markov state models • membrane permeability • molecular dynamics

- [1] a) E. M. Driggers, S. P. Hale, J. Lee, N. K. Terrett, *Nat. Rev. Drug Discovery* **2008**, *7*, 608–624; b) W. S. Horne, *Expert Opin. Drug Discovery* **2011**, *6*, 1247–1262; c) E. Marsault, M. L. Peterson, *J. Med. Chem.* **2011**, *54*, 1961–2004; d) J. Mallinson, I. Collins, *Future Med. Chem.* **2012**, *4*, 1409–1438; e) E. A. Villar, D. Beglov, S. Chennamadhavuni, J. A. Porco, D. Kozakov, S. Vajda, A. Whitty, *Nat. Chem. Biol.* **2014**, *10*, 723–731; f) A. K. Yudin, *Chem. Sci.* **2015**, *6*, 30–49; g) B. C. Doak, J. Zheng, D. Dobritzsch, J. Kihlberg, *J. Med. Chem.* **2016**, *59*, 2312–2327.
- [2] C. A. Lipinski, F. Lombardo, B. W. Dominy, P. J. Feeney, *Adv. Drug Delivery Rev.* **2001**, *46*, 3–26.
- [3] C. A. Lipinski, *J. Pharmacol. Toxicol.* **2000**, *44*, 235–249.
- [4] G. L. Amidon, H. J. Lee, *Annu. Rev. Pharmacol. Toxicol.* **1994**, *34*, 321–341.
- [5] A. C. Rand, et al., *Med. Chem. Commun.* **2012**, *3*, 1282–1289.
- [6] C. K. Wang, D. J. Craik, *Peptide Sci.* **2016**, *106*, 901–909.
- [7] A. R. Katritzky, M. Kuanar, S. Slavov, C. D. Hall, M. Karelson, I. Kahn, D. A. Dobchev, *Chem. Rev.* **2010**, *110*, 5714–5789.
- [8] a) J. M. Diamond, Y. Katz, *J. Membr. Biol.* **1974**, *17*, 121–154; b) A. Walter, J. Gutknecht, *J. Membr. Biol.* **1986**, *90*, 207–217; c) S. J. Marrink, H. J. C. Berendsen, *J. Phys. Chem.* **1994**, *98*, 4155–4168; d) S. J. Marrink, H. J. C. Berendsen, *J. Phys. Chem.* **1996**, *100*, 16729–16738.
- [9] D. Bemporad, J. W. Essex, C. Luttmann, *J. Phys. Chem. B* **2004**, *108*, 4875–4884.
- [10] D. Bemporad, C. Luttmann, J. W. Essex, *Biophys. J.* **2004**, *87*, 1–13.
- [11] C. T. Lee, J. Comer, C. Herndon, N. Leung, A. Pavlova, R. V. Swift, C. Tung, C. N. Rowley, R. E. Amaro, C. Chipot, Y. Wang, J. C. Gumbart, *J. Chem. Inf. Model.* **2016**, *56*, 721–733.
- [12] J. Comer, K. Schulten, C. Chipot, *J. Chem. Theory Comput.* **2014**, *10*, 2710–2718.
- [13] C. Chipot, J. Comer, *Sci. Rep.* **2016**, *6*, 35913.
- [14] *Cyclosporin A* (Ed.: D. J. G. White), Elsevier, Amsterdam, **1982**.
- [15] a) T. Rezai, B. Yu, G. L. Milhauser, M. P. Jacobson, R. S. Lockey, *J. Am. Chem. Soc.* **2006**, *128*, 2510–2511; b) T. Rezai, J. E. Bock, M. V. Zhou, C. Kalyanaraman, R. S. Lockey, M. P. Jacobson, *J. Am. Chem. Soc.* **2006**, *128*, 14073–14080.
- [16] K. Kajitani, M. Fujihashi, Y. Kobayashi, S. Shimizu, Y. Tsujimoto, K. Miki, *Proteins Struct. Funct. Bioinf.* **2008**, *70*, 1635–1639.
- [17] H.-R. Loosli, H. Kessler, H. Oshkinat, H.-P. Weber, T. J. Petcher, A. Widmer, *Helv. Chim. Acta* **1985**, *68*, 682–704.
- [18] S. S. F. Leung, J. Mijalkovic, K. Borrelli, M. P. Jacobson, *J. Chem. Inf. Model.* **2012**, *52*, 1621–1636.
- [19] S. S. F. Leung, D. Sindhikara, M. P. Jacobson, *J. Chem. Inf. Model.* **2016**, *56*, 924–929.
- [20] J. Witek, B. G. Keller, M. Blatter, A. Meissner, T. Wagner, S. Riniker, *J. Chem. Inf. Model.* **2016**, *56*, 1547–1562.
- [21] a) C. Schütte, A. Fischer, W. Huisinga, P. Deuffhard, *J. Comput. Phys.* **1999**, *151*, 146–168; b) W. C. Swope, J. W. Pitera, F. Suits, *J. Phys. Chem. B* **2004**, *108*, 6571–6581; c) J.-H. Prinz, H. Wu, M. Sarich, B. Keller, M. Senne, M. Held, J. D. Chodera, C. Schütte, F. Noé, *J. Chem. Phys.* **2011**, *134*, 174105; d) O. Lemke, B. G. Keller, *J. Chem. Phys.* **2016**, *145*, 164104.
- [22] The time scales of the interconversion rates in the MSMs of CsA are only rough estimates due to inaccuracies in the force field, finite sampling and discretization errors. For a detailed discussion, see F. Vitalini, et al., *J. Chem. Phys.* **2015**, *142*, 084101; Ref. [21c]; M. Sarich, et al., *Multiscale Model. Simul.* **2010**, *8*, 1154–1177.
- [23] Y. Rojas-Aguirre, J. L. Medina-Franco, *Mol. Diversity* **2014**, *18*, 599–610.
- [24] C. L. Ahlback, K. W. Lexa, A. T. Bockus, V. Chen, P. Crews, M. P. Jacobson, R. S. Lockey, *Future Med. Chem.* **2015**, *7*, 2121–2130.
- [25] M. Hušák, B. Kratochvíl, M. Buchta, L. Cvak, A. Jegorov, *Collect. Czech. Chem.* **1998**, *63*, 115–120.
- [26] N. Schmid, C. D. Christ, M. Christen, A. P. Eichenberger, W. F. van Gunsteren, *Comput. Phys. Commun.* **2012**, *183*, 890–903.
- [27] N. Schmid, A. P. Eichenberger, A. Choutko, S. Riniker, M. Winger, A. E. Mark, W. F. van Gunsteren, *Eur. Biophys. J.* **2011**, *40*, 843–856.
- [28] a) C. J. Woods, J. W. Essex, M. A. King, *J. Phys. Chem. B* **2003**, *107*, 13703–13710; b) U. H. E. Hansmann, *Chem. Phys. Lett.* **1997**, *281*, 140–150.
- [29] J. Witek, B. G. Keller, M. Blatter, A. Meissner, T. Wagner, S. Riniker, *J. Chem. Inf. Model.* **2017**, *57*, 2393–2393.
- [30] G. Ottaviani, S. Martel, P.-A. Carrupt, *J. Med. Chem.* **2006**, *49*, 3948–3954.

Manuscript received: September 11, 2017

Accepted manuscript online: September 18, 2017

Version of record online: November 2, 2017